The use of high-energy synchrotron diffraction for residual stress analyses

W. REIMERS, A. PYZALLA, M. BRODA, G. BRUSCH, D. DANTZ, T. SCHMACKERS
Hahn-Meitner-Institut, Glienicker Strasse 100, D-14109 Berlin, Germany
E-mail: pyzalla@hmi.de

K.-D. LISS
European Synchrotron Radiation Facility ESRF, B.P. 220, F-38043 Grenoble Cédex, France

T. TSCHENTSCHER
DESY, HASYLAB, Notkestraße 85, D-22603 Hamburg, Germany

Residual stresses are formed due to inhomogeneous deformation gradients or temperature fields during the manufacturing and processing of components. In superposition with load stresses, they severely influence the strength and failure of components. For the non-destructive evaluation of the residual stresses in crystalline materials, well-developed angle dispersive methods for X-ray residual stress analysis exist at the surface and neutron residual stress analysis in the bulk of components [1–3].

Energy dispersive methods are employed in the case of neutron residual stress analysis at pulsed reactors and spallation sources using a time-of-flight approach. First attempts at using energy dispersive methods in synchrotron diffraction ($E < 50$ keV) for residual stress analysis have been relinquished due to the poor resolution of Ge-detectors at that time [4, 5]. Today, improvements in the detectors and in the evaluation methods for the determination of the line position enable energy dispersive X-ray diffraction, which reaches penetration depths up to several mm but requires gauge volumes of the order of several mm^3 [6]. Encouraged by this, recent experiments at the high-energy beam line ID15A in Grenoble, France, were performed, which revealed that residual stress analysis with a gauge volume more than one dimension smaller can be performed using high-energy synchrotron diffraction (HESD). The high-energy diffraction beam line ID15A of the European Synchrotron Radiation Facility in Grenoble, France, has an energy range up to $E =$ 1000 keV. The measurements were performed using an 80 μm slit in the incoming beam and two 100 μm slits in the reflected beam. The diffraction angle was kept constant at $2\theta = 10°$. Thus, the gauge volume is a parallelpiped with a length of 1650 μm and a width of 145 μm (Fig. 1). After identifying the reflection, the lattice spacing d^{hkl} can be calculated according to Bragg's law, which can be written as a function of the energy E^{hkl}:

$$d^{hkl} = \frac{hc}{2 \sin \theta} \cdot \frac{1}{\mathrm{E}^{hkl}} = \text{const.} \cdot \frac{1}{E^{hkl}} \qquad (1)$$

where hkl denote the Miller's indices, θ is the Bragg angle, h is Planck's constant and c is the velocity of light. The strain $\varepsilon_{\phi\psi}$ at the sample orientation ϕ, ψ is evaluated from the shift of the lattice spacing:

$$\varepsilon_{\phi\psi}^{hkl} = \frac{d_{\phi\psi}^{hkl}}{d_0} - 1 = \frac{E_0}{E_{\phi\psi}^{hkl}} - 1 \qquad (2)$$

where d_0 denotes the lattice parameter of the stress-free material and E_0 is the corresponding energy value. Strain measurement in different directions of the samples allows for the determination of the strain tensor ε. The stress tensor σ can then be calculated from the strain tensor ε using Hooke's law, taking into account the diffraction elastic constants (DEC):

$$\sigma = \underline{\underline{\mathrm{E}}}(\mathrm{DEC})\varepsilon \qquad (3)$$

The main advantages of using HESD, which are the high penetration depth, the high local resolution achievable due to the high intensity and paralleleism of the beam as well as the energy dispersive characteristic allowing for the simultaneous analysis of residual stresses and texture, are illustrated in three examples, namely a ceramic matrix composite (CMC), a thermal barrier coating (TBC) and a cold-forward-extruded steel sample.

In a fiber-reinforced composite, C/SiC–composite residual stresses arise due to the shrinkage of the matrix material during the pyrolytical manufacturing process and due to the mismatch of the coefficient of thermal expansion (CTE) of the fibers and the matrix. The composite has a laminate structure where each layer of fibers is unidirectional. Here, the layers were 250 μm thick and shifted alternately around 90°. The aim of the HESD analysis was to determine the residual stresses parallel and perpen-

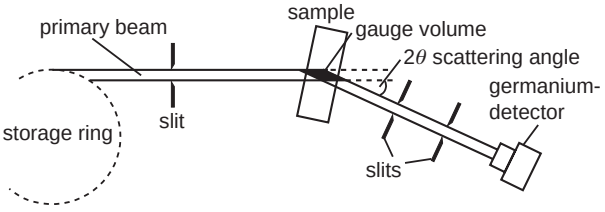

Figure 1 Experimental set-up at the beam line ID15A at the ESRF, Grenoble, France.

0261-8028

dicular to the fibers within a layer in the bulk of the sample. The penetration depth combined with the resolution necessary for this task cannot be achieved using X-ray or neutron diffraction but can be by employing HESD. Due to the high thermal expansion mismatch of the matrix and the fiber, which even has a negative thermal expansion coefficient in the direction of the fiber axis, the matrix contains high tensile residual stresses in fiber direction (Fig. 2). Perpendicular to the fiber axis, the thermal mismatch is lower and thus the matrix residual stresses almost vanish in this direction.

Another example of the possibilities that arise from the high intensity and penetration depth of the high-energy synchrotron beam is the determination of residual stresses in small layers on shallow buried interfaces. The residual stresses of a duplex thermal barrier coating system consisting of a plasma-sprayed ZrO_2-7 wt% Y_2O_3 ceramic layer with a thickness of 0.5 mm and a NiCoCrAlY bond layer with a thickness of 0.15 mm, both deposited on a superalloy In 718 substrate with a thickness of 2 mm (Fig. 3), were determined by HESD. In this TBC, the residual stresses in the bond layer are of special interest. This layer is buried between the ceramic layer and the substrate and is thus not accessible by X-ray. Also, the residual stresses in the bond layer cannot be determined by neutrons due to the small layer thickness. Here, HESD in the NiCoCrAlY bond layer allowed the determination of the residual stress change due to different external loads for the first time. To analyze the stress state of the bond coat between the ceramic layer and the substrate and its dependence on an applied load, a four-point bending device was used. The measurements were performed first without load and then at two different load levels (93 N and 140 N). Within the ceramic layer, good agreement (Fig. 4) was found between the residual stress values determined by X-ray, HESD and calculations based on a multilayer model [7]. Also, within the bond coat that is not accessible to X-ray, the residual stress values calculated and those experimentally determined by HESD agree well.

Besides the benefits arising from the high penetration depth and the high intensity of the high-energy synchrotron radiation, the simultaneous determination of residual stresses and texture is an advantage of the energy dispersive arrangement. In a full-forward-extruded sample (Fig. 5), German steel grade C15, degree of natural strain $\varphi = 1.2$, residual stress and texture gradients arise due to strong plastic deformations, which are inhomogeneously distributed across the sample diameter. Therefore, several volume elements had to be investigated across the sample diameter. The energy spectra obtained in the direction parallel and perpendicular to the axis of the sample reveal a typical $\langle 1\,1\,0 \rangle$ fiber texture. A comparison of the intensity of the 1 1 0-type reflections for the different volume elements across the sample diameter shows that the

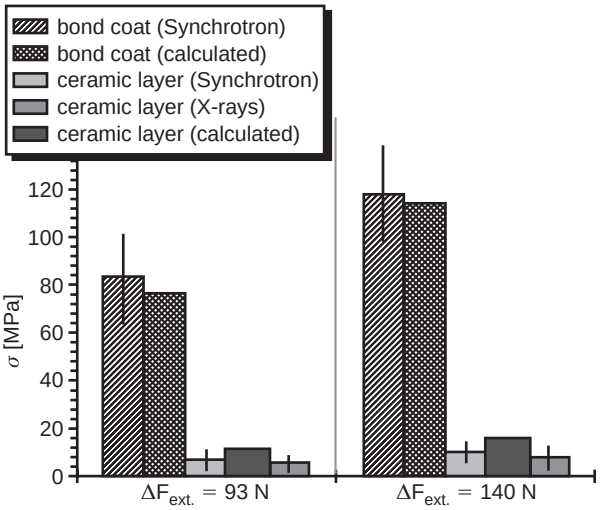

Figure 4 Residual stresses in the bond coat and the ceramic layer of a TBC.

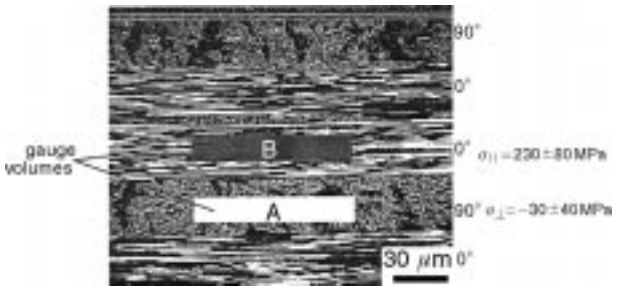

Figure 2 Residual stresses parallel and perpendicular to the C fibers in the SiC matrix of a C/SiC–composite.

Figure 3 Thermal barrier coating.

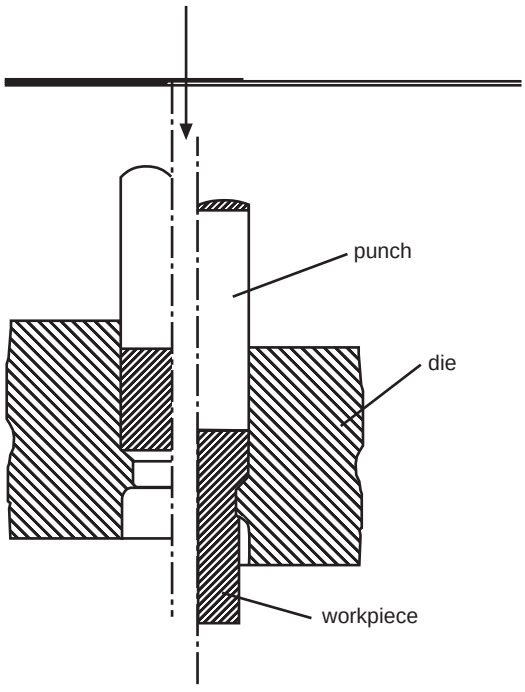

Figure 5 Full-forward-extruded steel sample.

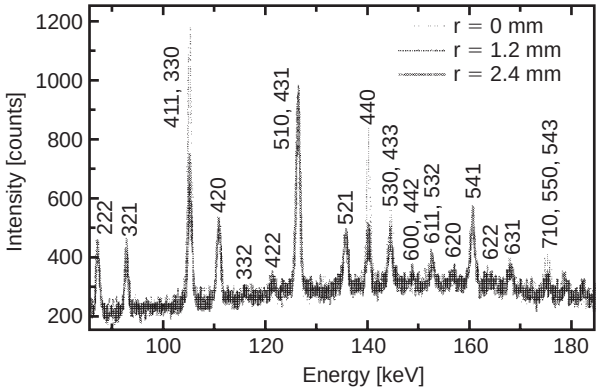

Figure 6 Energy spectrum of a full-forward-extruded steel sample ($r = 0$: center of the sample, sample diameter 15 mm).

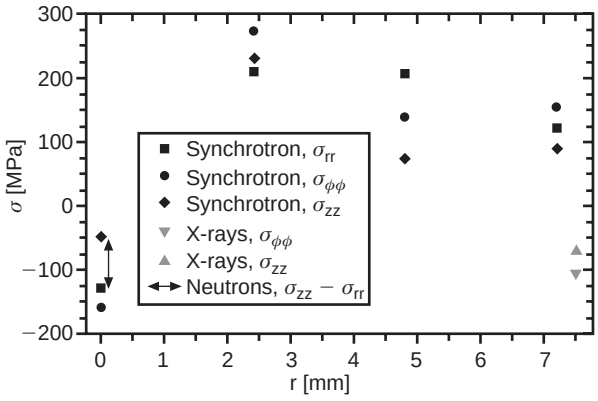

Figure 7 Residual stresses in a full-forward-extruded steel sample.

maximum of the texture is in the center of the sample and that the texture is distinctly less pronounced near the sample boundary (Fig. 6). Thus, it can be concluded that the plastic deformation is concentrated in the rod kernel, which corresponds to the X-ray pole figure and theoretical analyses [8, 9]. From the energy values, the residual stresses were calculated at the different positions of the gauge volume. The d_0 value necessary to determine the three-dimensional residual stress state was calculated as an average of all d values measured. Neutron diffraction and synchrotron diffraction, in very good agreement, reveal that in the inner part of the specimen the residual stresses in radial σ_{rr}, hoop $\sigma_{\phi\phi}$ and axial direction σ_{zz} are compressive (Fig. 7). These compressive residual stresses are balanced by tensile residual stresses in the outer part of the sample. The quantitative stress values also fulfill, within an experimental error margin of ± 80 MPa, the mechanical equilibrium condition.

From the examples of high-energy dispersive synchrotron residual stress analysis on a CMC, a TBC and a textured sample it can be concluded that this new method in comparison to X-ray, neutron and conventional synchrotron diffraction has strong advantages with respect to the high penetration depth and the high local resolution achievable, as well as to the simultaneous investigation of residual stresses and texture.

Acknowledgment

The authors would like to thank the European Synchrotron Radiation Facility (ESRF) for the allocation of beam time.

References

1. V. HAUK and E. MACHERAUCH *Adv. X-ray Analysis* **27** (1989) 81.
2. L. PINTSCHOVIUS, in "Measurement of residual and applied stress using neutron diffraction", edited by M. Hutchings and A. Krawitz (Kluwer Academic Publishers, Dordrecht, 1989) p. 115.
3. A. J. ALLEN, M. T. HUTCHINGS, C. G. WINDSOR and C. ANDREANI, *Adv. Physics* **34** (1985) 445.
4. H. RUPPERSBERG, *Adv. X-Ray Analysis* **35** (1992) 481.
5. H. RUPPERSBERG and I. DETEMPLE, *Mater. Sci. Engng.* **A161** (1993) 41.
6. G. BRUSCH and W. REIMERS, "Proceedings of the ICRS 5 Linköping, Sweden, 1997" to be published.
7. O. T. IANCU and D. MUNZ, *J. Amer. Ceram. Soc.* **73** (1990) 1144.
8. A. E. TEKKAYA, Ph.D. Thesis, Universität Stuttgart (1986).
9. A. PYZALLA and W. REIMERS, in "Competitive advantages by near-net-shape manufacturing", edited by H.-D. Kunze (DGM–Informationsgesellschaft, Verlag, Oberursel 1997) p. 175.

Received 15 July
and accepted 28 August 1998